

Loss of Mitofusin 2 Promotes Endoplasmic Reticulum Stress*

Received for publication, March 5, 2012, and in revised form, April 6, 2012. Published, JBC Papers in Press, April 17, 2012, DOI 10.1074/jbc.M112.359174

Gladys A. Ngoh, Kyriakos N. Papanicolaou, and Kenneth Walsh¹

From the Whitaker Cardiovascular Institute, Boston University School of Medicine, Boston, Massachusetts 02118

Background: The role of Mfn2 in ER stress has not been examined previously.

Results: ER stress up-regulates Mfn2. Ablation of Mfn2 delays translational recovery, alters late UPR signaling, and increases cell death during ER stress.

Conclusion: Mfn2 influences whether the UPR is adaptive or apoptotic.

Significance: Mfn2 is an ER stress-inducible factor that contributes to ER homeostasis.

The outer mitochondrial membrane GTPase mitofusin 2 (Mfn2) is known to regulate endoplasmic reticulum (ER) shape in addition to its mitochondrial fusion effects. However, its role in ER stress is unknown. We report here that induction of ER stress with either thapsigargin or tunicamycin in mouse embryonic fibroblasts leads to up-regulation of Mfn2 mRNA and protein levels with no change in the expression of the mitochondrial shaping factors Mfn1, Opa1, Drp1, and Fis1. Genetic deletion of Mfn2 but not Mfn1 in mouse embryonic fibroblasts or cardiac myocytes in mice led to an increase in the expression of the ER chaperone proteins. Genetic ablation of Mfn2 in mouse embryonic fibroblasts amplified ER stress and exacerbated ER stress-induced apoptosis. Deletion of Mfn2 delayed translational recovery through prolonged eIF2 α phosphorylation associated with decreased GADD34 and p58^{IPK} expression and elevated C/EBP homologous protein induction at late time points. These changes in the unfolded protein response were coupled to increased cell death reflected by augmented caspase 3/7 activity, lactate dehydrogenase release from cells, and an increase in propidium iodide-positive nuclei in response to thapsigargin or tunicamycin treatment. In contrast, genetic deletion of Mfn1 did not affect ER stress-mediated increase in ER chaperone synthesis or eIF2 α phosphorylation. Additionally, ER stress-induced C/EBP homologous protein, GADD34, and p58^{IPK} induction and cell death were not affected by loss of Mfn1. We conclude that Mfn2 but not Mfn1 is an ER stress-inducible protein that is required for the proper temporal sequence of the ER stress response.

The endoplasmic reticulum (ER)² is a highly dynamic organelle consisting of interconnected tubules involved in the synthesis, folding, and transport of secretory and membrane proteins (1). It also serves as a site for calcium storage (2).

* This work was supported, in whole or in part, by National Institutes of Health Grants HL102874, AG34972, AG15052, and HL68758 (to K. W.). This work was also supported by a postdoctoral fellowship on T32 Training Grant HL007224 to the Whitaker Cardiovascular Institute (to G. N.).

¹ To whom correspondence should be addressed: Whitaker Cardiovascular Institute, Boston University School of Medicine, 715 Albany St., W611, Boston, MA 02118. Tel.: 617-414-2390; Fax: 617-414-2391; E-mail: kxwalsh@bu.edu.

² The abbreviations used are: ER, endoplasmic reticulum; UPR, unfolded protein response; TG, thapsigargin; TM, tunicamycin; PERK, protein kinase-like endoplasmic reticulum kinase; CHOP, C/EBP homologous protein; MEF, mouse embryonic fibroblast; PI, propidium iodide.

Perturbing the protein synthetic machinery or ER Ca²⁺ homeostasis will induce a condition that is referred to as ER stress (3, 4). ER stress activates complex cytoplasmic and nuclear signaling pathways, collectively called the unfolded protein response (UPR) (5). Initially, the UPR seeks to reestablish ER homeostasis via translational attenuation to decrease ER load, transcriptional activation of chaperone genes to increase the folding capacity of the ER, and activation of the ER-associated degradation machinery to clear misfolded proteins (6–8). If ER stress is unresolved, apoptosis is triggered (9, 10). ER stress is linked to the pathophysiology of numerous diseases, including diabetes, atherosclerosis, and Alzheimer's disease (11–13). Experimentally, ER stress can be induced by tunicamycin, which inhibits N-glycosylation of nascent ER proteins by preventing UDP-GlcNAc-dolichol phosphate GlcNAc-phosphate transferase activity (14), or thapsigargin (TG), which inhibits ER Ca²⁺ ATPase, leading to the depletion of ER calcium stores (15).

Three ER transmembrane proteins are instrumental in coordinating the UPR signal. These proteins are inositol-requiring transmembrane kinase and endoribonuclease 1 α (IRE1 α), activation transcription factor 6 (ATF6), and protein kinase-like ER kinase (PERK). In response to ER stress, IRE1 α catalyzes Xbp1 mRNA splicing, leading to the generation of an active transcription factor that translocates to the nucleus and activates the transcription of genes involved in protein folding and degradation to restore ER homeostasis (16). ATF6 is transported to the Golgi complex, where it is cleaved by proteases to yield a transcription factor that activates the expression of genes involved in protein folding (17, 18). In addition to this transcriptional regulation, PERK phosphorylates eukaryotic initiation factor 2 α (eIF2 α), leading to the rapid attenuation of protein translation (7, 19–21). This translational attenuation is transient because the production of proteins required for increased ER capacity is required during the later phase of the stress response. Thus, during the late phase, the stress-induced phosphatase GADD34 and the PERK inhibitor P58^{IPK} mediate the dephosphorylation of eIF2 α to restore protein translation (22, 23). Ultimately, if the ER stress is not mitigated, eIF2 α phosphorylation promotes apoptosis through the induction of C/EBP homologous protein (CHOP).

The mitofusins, Mfn1 and Mfn2 are transmembrane GTPases located on the outer mitochondrial membrane (OMM) that participate in the fusion of this organelle (24).

Mfn2 and ER Stress

Complete ablation of either mitofusin protein leads to embryonic lethality in mice, whereas mutations in human *MFN2* are associated with Charcot-Marie-Tooth type IIa, a peripheral neuropathy (25, 26). It has been reported that mitofusins are required for neuronal function and for maintenance mitochondrial DNA (mtDNA) in skeletal muscle of mice (27, 28). Recently, the targeted ablation of either Mfn1 or Mfn2 in cardiac myocytes was shown to result in the diminution or enlargement of mitochondrial size, respectively, with little or no deterioration of cardiac function (29, 30). Loss of either Mfn1 or Mfn2 delays oxidative stress-induced loss of mitochondrial membrane potential and mitochondrial permeability transition pore activation. In contrast, the simultaneous ablation of both mitofusins in cardiac myocytes leads to severe cardiac dysfunction and gross deformities in mitochondrial structure (31).

Although Mfn1 and Mfn2 are highly homologous, studies have shown that they are not entirely redundant. In this regard, Mfn2 has been shown to exert extramitochondrial functions (32). Mfn2 differs from Mfn1 in that it is also present in the ER where it regulates ER shape, tethers ER and mitochondria, and regulates mitochondrial uptake of Ca^{2+} released by the ER (33). This study also demonstrates that the mutations in *MFN2* associated with Charcot-Marie-Tooth type IIa syndrome selectively affect ER tubulation and tethering to the mitochondria. Ablation of the Mfn2 gene has also been shown to uncouple mitochondria from the ER, increasing the distance between these organelles in cultured cells and interfering with interorganelle Ca^{2+} transport (33). In contrast, the sarcoplasmic reticulum-mitochondria distance is not affected when Mfn2 was ablated in adult cardiac myocytes, where these structures appear to be locked into a tight crystalline-like array (29).

In this work, we provide evidence for the first time that Mfn2 but not Mfn1 is up-regulated upon the induction of ER stress. Moreover, ablation of Mfn2 but not Mfn1 in cultured mouse embryonic fibroblasts (MEFs) or adult cardiac myocytes *in vivo* led to an up-regulation of ER chaperone proteins both at baseline and in response to treatment with TG or TM in MEFs. Loss of Mfn2 was found to sensitize cells to ER stress-induced cell death by increasing caspase activity and augmenting CHOP induction. These findings suggest that Mfn2 but not Mfn1 is an ER stress regulatory protein that is necessary for the homeostasis of the ER.

EXPERIMENTAL PROCEDURES

Isolation and Culture of Primary Mouse Embryonic Fibroblasts—Primary MEFs were isolated in accordance with the University of Boston Animal Care and Use Committee. Using a protocol modified from Kamijo *et al.* (34), pregnant female mice with either loxP-flanked Mfn1 or loxP-flanked Mfn2 genes were sacrificed on embryonic day 14.5 of gestation by CO_2 asphyxiation, and mouse embryos were explanted. Following removal of the head, heart, and liver, embryos were rinsed with phosphate-buffered saline, minced, and digested with trypsin (0.25% solution containing 0.5 mM EDTA) for 15 min at 37 °C using 3 ml per embryo. Trypsin was inactivated by addition of DMEM containing 10% fetal bovine serum and penicillin/streptomycin. Cells from embryos were plated into 150-mm diameter culture dishes and incubated at 37 °C in a 5% CO_2 -humidified chamber. Plating after disaggregation of embryo cells was

considered passage 1. Cells were then subcultured in 35-mm dishes and 6- or 12-well plates for experimentation.

Adenoviral Transfection—MEFs were transfected with 50 multiplicity of infection of replication-deficient adenoviruses carrying the cre recombinase gene (AdCre), Null gene (AdNull), or green fluorescent protein (AdGFP) for 48 or 72 h. Viruses were purchased from Vector Biolabs. Adenoviruses were delivered to the cells for 4 h, and then the medium was changed to fresh DMEM. The cells were transfected with adenovirus 24 or 48 h before treatment with thapsigargin or tunicamycin at the indicated concentrations to induce ER stress. Functional expression was confirmed by appropriate immunoblot analysis or real-time PCR. Transfection efficiency using these conditions was about 80%. Sample size is equal to at least five per group per treatment.

ER Stress Induction—MEFs treated as mentioned above were subjected to ER stress by treatment with 0.1 $\mu\text{mol/L}$ of TG (for 0.5 or 18 h) or 0.5 $\mu\text{g/ml}$ of TM (for 1 or 18 h). In the case of TG, after 0.5 h of TG treatment, medium was changed to fresh DMEM, and cells were allowed to recover. TM inhibits *N*-glycosylation of nascent ER proteins (14), whereas TG depletes ER calcium stores by inhibiting ER Ca^{2+} ATPase (15).

Cardiac Myocyte-specific Ablation of Mfn1 and Mfn2 in Mice—Mice with cardiac myocyte specific deletion of Mfn1 (Mfn1 CKO) and Mfn2 (Mfn2 CKO) were generated as described previously (29, 30), and mice were handled according to the regulations of the Institutional Animal Care and Use Committee of Boston University School of Medicine.

Protein Extraction—Total cellular proteins were isolated from MEFs treated as mentioned above. Monolayer cultures of MEFs were washed with PBS, harvested in ice-cold lysis buffer (containing 20 mmol/liter Tris-HCl, 150 mmol/liter NaCl, 1 mmol/liter Na_2EDTA , 1 mmol/liter EGTA, 1% (v/v) Triton, 2.5 mmol/liter sodium pyrophosphate, 1 mmol/liter glycerophosphate, 1 mmol/liter Na_3VO_4 , 1 $\mu\text{g/ml}$ leupeptin, 0.1% (v/v) protease inhibitor mixture, and 1 mmol/liter PMSF) using a cell scraper. Extracts were sonicated, and the resulting lysates were centrifuged at $15,000 \times g$ for 5 min at 4 °C to remove cell debris. Total protein was estimated using bicinchoninic acid assay. Lysates were immediately frozen in liquid nitrogen and stored at -80 °C until used. Total cellular protein was also isolated from hearts of WT, Mfn2 CKO, and Mfn1 CKO mice as described previously (30).

Western Blotting—Twenty-five μg of protein was applied to each lane of a 10% Tris-glycine SDS-PAGE gel and electroblotted onto PVDF membranes. Reagent-grade nonfat milk (Bio-Rad) 5% (w/v) in Tris-buffered saline was used for blocking. Blots were incubated with anti-Mfn2 (1:2000, Sigma), anti-Mfn1 (1:1000, NeuroMab), anti-Grp94 (1:4000, Santa Cruz Biotechnology), anti-Grp78 (1:1000, Santa Cruz Biotechnology), anti-CHOP (1:1000; Santa Cruz Biotechnology), anti-GADD34 (1:1000, Santa Cruz Biotechnology), anti-p-eIF2 α (1:1000, Cell Signaling Technology), anti-eIF2 α (1:2000, Cell Signaling Technology), anti-p58^{IPK} (1:2000, Cell Signaling Technology) or α -tubulin (1:2000, Cell Signaling Technology) as primary antibodies overnight at 4 °C. Blots were then incubated for 1 h with 0.1 $\mu\text{g/ml}$ of secondary antibody (goat anti-rabbit IgG-HRP-conjugated, goat anti-mouse IgG-HRP-conju-

gated, goat anti-rat IgG-HRP-conjugated) and detected with an enhanced chemiluminescent detection system (Pierce). Densitometry was performed using non-saturated chemiluminescent membranes exposed using a Fuji LAS-4000 bio-imaging analyzer and quantified using ImageJ software. Multiple exposures from every experiment were used to confirm that the signal was within the linear range. Levels of proteins of interest were normalized to α -tubulin and then expressed as a percentage of control (set at 100%).

PCR—Total RNA was extracted with TRIzol reagent (Invitrogen). Total RNA (1 μ g) was subjected to reverse transcriptase reaction to synthesize the cDNA using SuperScriptTM III first-stand synthesis system (Invitrogen). Quantification of cDNAs was by real-time PCR using SYBR Green (Applied Biosystems). These quantities were expressed relatively to that of the *Gapdh* gene. All primer sequences for genes shown are available upon request. All primers were purchased from Integrated DNA Technologies.

Assessment of ER and Mitochondrial Morphology—ER and mitochondrial morphology was evaluated in Mfn2^{loxP} MEFs cultured on 3-mm glass bottom dishes (MatTak). MEFs were transfected with AdCre to ablate Mfn2 or treated with 0.1 μ M TG for 18 h to induce ER stress. MEFs were then transfected with either a vector encoding the ER targeting sequence of calreticulin fused to the 5' end of DsRed2 (Clontech) to evaluate ER morphology or stained with 100 nM MitoTracker Green (Molecular Probes) to evaluate mitochondrial morphology. Using confocal microscopy, DsRed2 was excited with the 543-nm laser set at 40% power, whereas MitoTracker Green was excited with the 488-nm laser set at 7% power and visualized with a $\times 63$ oil immersion lens (Plan-Apochromat, NA 1.5). All experimental groups were repeated three times.

Cell Death Assays—Cell death was assessed for MEFs by measuring lactate dehydrogenase (LDH) release spectrophotometrically using a commercially available kit (Sigma) following ER stress induction. The results were expressed as LDH release relative to total LDH in the cells and normalized to untreated control. Similarly treated MEFs were also stained with the fluorescent DNA-binding dyes DAPI (10 μ g/ml) and propidium iodide (PI, 10 μ g/ml) for 1 h, similar to previous work (35, 36). The stained nuclei were then visualized using a LUCPlanApo $\times 10/0.4$ objective on an Olympus inverted fluorescence microscope and Xcite 120 Fluor light source (level of 12%). Filters used included 350/50 nm excitation and 470/40 nm emission filters for DAPI and 560/40 nm excitation and 630/60 nm emission filters for PI. Exposure duration was set at 100 ms for DAPI and 500 ms for PI. Four fields per treatment were counted, treatments were done in duplicates, and data were expressed as percent PI-positive nuclei/total nuclei. Sample size was equal to six per group per treatment. Apoptosis was also assessed by measuring caspase-3/7 activity in whole cell lysates using the Caspase Glo kit (Promega) according to the instructions of the manufacturer. Briefly, equal volumes of whole cell lysate (30 μ g) and caspase reagent were mixed and incubated in the dark for 1 h at room temperature. Bioluminescence was measured using an Infinite[®] M1000 microplate reader (TECAN) and expressed in percent luminescence (normalized to control). Sample size was equal five per group per treatment.

Statistical Analysis—Results are shown as mean \pm S.E. The statistical analysis (Graph Pad 4.0) was conducted using Student's *t* test or by one-way analysis of variance followed by Dunnett's test, as appropriate. Differences were considered statistically significant if $p < 0.05$.

RESULTS

Mfn2 Is Up-regulated by ER Stress—To establish a link between ER stress and the expression of proteins involved in mitochondrial dynamics, MEFs were treated with TG (0.1 μ mol/liter), which depletes ER Ca²⁺, or TM (0.5 μ g/ μ l), which inhibits ER N-glycosylation, for 18 h to induce ER stress. Treatment with TG induced Mfn2 transcript levels 1.9-fold ($p < 0.05$) and TM induced Mfn2 transcript levels by 1.8-fold ($p < 0.05$), as determined by quantitative real-time PCR (Fig. 1A). Neither TG- nor TM-induced ER stress altered the transcript levels of other outer mitochondrial membrane fusion protein Mfn1. Furthermore, these agents did not influence the transcript levels of other proteins involved in mitochondrial fission and fusion including Opa1, Drp1, or Fis1. Treatment of MEFs with TG or TM also led to the up-regulation of Mfn2 but not Mfn1 protein levels by a factor of 2 (Fig. 1B). The induction of Mfn2 paralleled the increase in the levels of the ER chaperone proteins Grp78 and Grp94. Taken together, the above results suggest that among mitochondrial fission and fusion proteins, Mfn2 is selectively up-regulated by ER stressors.

Ablation of Mfn2 Augments ER Chaperone Expression—The accumulation of unfolded proteins in the ER lumen induces the selective induction of chaperone proteins (21). To determine whether Mfn2 affects this arm of the UPR response, an adenoviral vector expressing cre recombinase (AdCre) was used to ablate Mfn2 by transducing MEFs isolated from Mfn2^{lox/lox} mice. The transfection efficiency for the AdCre was estimated to be greater than 75% on the basis of transfection with an adenoviral vector that expresses the GFP reporter gene (Fig. 2A). Forty eight h after transfecting primary MEFs with AdCre, total cellular proteins were harvested, and protein levels were evaluated via Western immunoblot analysis. Immunoblots for Mfn1 and Mfn2 showed significant reductions in Mfn2 but no change in Mfn1 levels compared with MEFs treated with a control adenovirus lacking the Cre transgene (*AdNull*) (Fig. 2B).

To determine the effects of Mfn2 ablation on the UPR, control and Mfn2-deficient MEFs were evaluated for ER chaperone protein expression under baseline conditions and in response to treatment with TG or TM. Ablation of Mfn2 augmented baseline Grp78 expression and, to a lesser extent, Grp94 expression (Fig. 2C). As expected, treatment with TG or TM led to increased expression of Grp78 and Grp94, and the induction of these proteins was generally higher in Mfn2-ablated MEFs compared with the control. Additionally, real-time PCR showed significantly up-regulated mRNA levels of ATF4 and Grp94 for AdCre-treated MEFs compared with the control MEFs at base line (Fig. 2D). In contrast, ablation of Mfn2 did not affect levels of calreticulin, either at base line or under ER stress conditions (data not shown). Mfn2 ablation did not affect mRNA levels of the mitochondrial fusion factors Mfn1 and Opa1, nor the expression of the mitochondrial fission factors Drp1 and Fis1 (Fig. 2D).

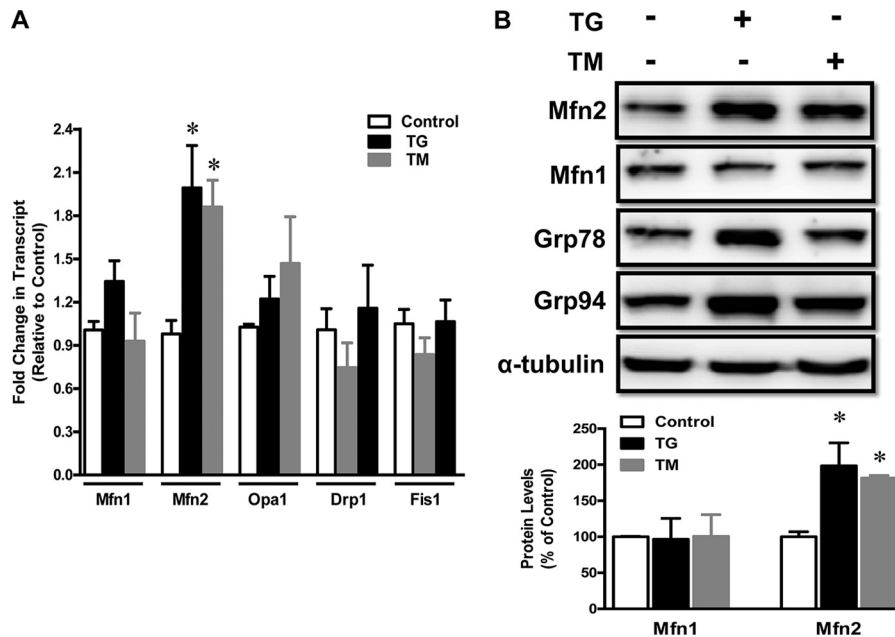


FIGURE 1. ER stress up-regulates Mfn2 expression in fibroblasts. MEFs were subjected to ER stress with 0.1 μ M TG or 0.5 μ g/ μ l TM for 18 h. *A*, real-time PCR was performed to determine the mRNA levels of mitochondrial fusion proteins (mitofusin 1 (*Mfn1*), mitofusin 2 (*Mfn2*), and optic atrophy 1 long variant (*Opa1*)) and mitochondrial fission proteins (dynamins-related protein (*Drp1*) and mitochondrial fission protein 1 (*Fis1*)). *B*, endogenous expression of mitochondrial fusion proteins (*Mfn1* and *Mfn2*) and of ER chaperones (*Grp78* and *Grp94*) determined by Western blotting and densitometric quantification of immunoblot analyses for Mfn1 and Mfn2. Results are expressed as mean \pm S.E.; $n = 5$ /group; *, $p < 0.05$ versus control.

In contrast to Mfn2 ablation, the selective ablation of Mfn1, achieved by treating Mfn1^{lox/flox} MEFs with AdCre (Fig. 3A), did not affect either baseline or ER stress-induced chaperone expression (Fig. 3B). Quantitative transcript analysis also did not reveal significant changes in the mRNA levels of factors involved with the regulation of mitochondrial fusion and fission (data not shown). Overall, the above results suggest a role for Mfn2 but not Mfn1 in ER stress signaling.

Loss of Mfn2 Alters ER and Mitochondrial Morphology—The effects of Mfn2 ablation and ER stress on mitochondria and ER shape were analyzed by confocal microscopy in Mfn2^{lox/flox} MEFs. In control MEFs, the ER appeared as interconnected networks. The induction of ER stress with TG or ablation of Mfn2 had similar effects on ER morphology, resulting in the formation of dilated and aggregated structures as shown by DsRed fluorescence (Fig. 4, upper panels). Similarly, both ER stress and ablation of Mfn2 resulted in similar alterations to the mitochondrial network. Although the mitochondrial structure was mostly tubular-like in control MEFs, mitochondria from MEFs subjected to ER stress or deficient in Mfn2 expression showed a fragmented phenotype, as shown by MitoTracker Green fluorescence (Fig. 4, lower panels).

Ablation of Mfn2 in Cardiac Myocytes in Vivo Augments ER Chaperone Expression—Mice with targeted deletion of either Mfn1 or Mfn2 in cardiac myocytes are viable and survive through adulthood (29, 30). Because Mfn2 ablation augments the expression of ER stress makers in MEFs, we sought to confirm these findings *in vivo* in mice with cardiac myocyte-specific deletion of Mfn2 (Mfn2 CKO mice). Although ablation of Mfn2 in the heart did not significantly change the expression of other mitochondrial fusion (Mfn1 and Opa1) or fission (Drp1 and Fis1) factor mRNA levels, the transcript levels for the ER stress response markers ATF4 and Grp94 were elevated signif-

icantly elevated in heart (Fig. 5A). Western blotting also revealed augmented expression of the UPR-inducible proteins Grp94 and Grp78, and a smaller but reproducible increase in calreticulin in hearts of Mfn2 CKO compared with WT mice (Fig. 5B). In contrast, cardiac myocyte-specific ablation of Mfn1 (Mfn1 CKO) did not affect the expression levels of Grp94, Grp78, or calreticulin (Fig. 5C).

Loss of Mfn2 Affects UPR Signaling—ER stress is associated with the temporal regulation of UPR proteins. Therefore, time course studies analyzing the expression of Mfn2 and known ER stress proteins were performed in MEFs treated with TG. Mfn2 up-regulation occurred in the late phase of ER stress (8 h) and was accompanied by increases in CHOP, Grp94, Grp78, GADD34, and p58IPK expression (Fig. 6, A and B). The up-regulation of Mfn2 was preceded by the transient up-regulation of eIF2 α phosphorylation.

Phosphorylation and dephosphorylation of eukaryotic initiation factor 2 (eIF2 α) is a critical early step in the regulation of protein synthesis during ER stress (20–23). Therefore, we determined whether loss of Mfn2 affects the phosphorylation status of eIF2 α during the early and late stages of the UPR. In the absence of ER stress, loss of Mfn2 did not affect baseline phosphorylation of eIF2 α (data not shown). In control MEFs, brief treatment with TG (0.5 h) or TM (1 h) was associated with a profound increase in eIF2 α phosphorylation (Fig. 6, C and D). This early increase in eIF2 α phosphorylation was not altered by the ablation of Mfn2. In contrast, levels of phosphorylated eIF2 α remained elevated at late time points (18 h) after treatment with TG or TM in Mfn2-ablated MEFs compared with control MEFs. An analysis of multiple time course experiments revealed that Mfn2 ablation led to 5.4 \pm 1.2-fold and 4.7 \pm 1.5-fold elevations in eIF2 α phosphorylation in TG- and TM-treated cells, respectively, at the 18-h time point ($p < 0.01$).

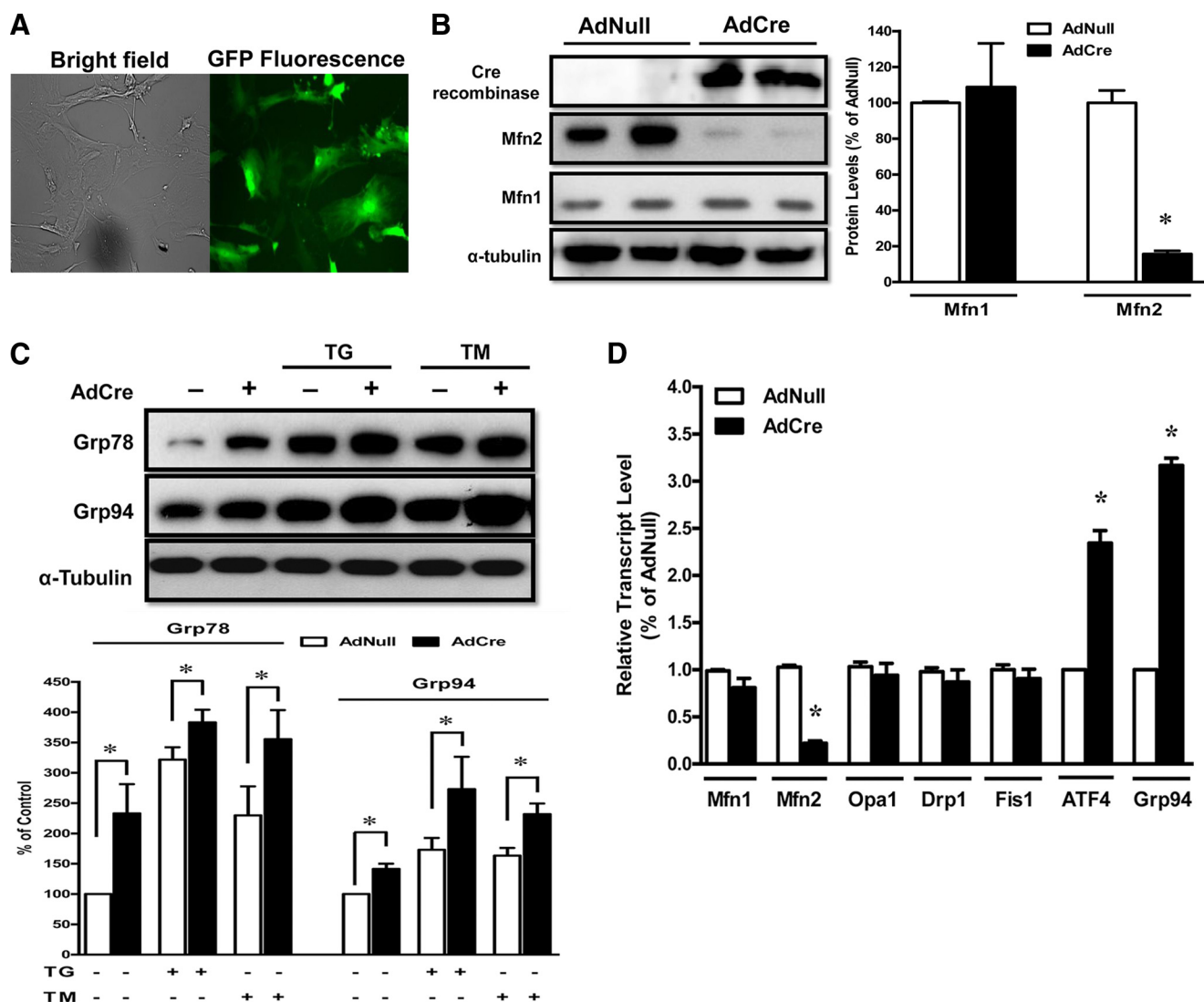


FIGURE 2. Ablation of Mfn2 in fibroblasts promotes ER chaperone protein expression. LoxP-flanked Mfn2 MEFs were transfected with an adenoviral vector-expressing Cre (*AdCre*) to delete *Mfn2* or control virus (*AdNull*) for 48 h. *A*, fluorescent microscopy was used to determine transfection efficiency in *AdCre*-transfected cells. Transfection efficiency was found to be greater than 75%. *B*, whole cell lysates were extracted from similarly treated MEFs and immunoblotted for Cre recombinase, Mfn1, and Mfn2. A representative immunoblot analysis is shown. Blots were quantified by densitometry, and levels of Mfn1 and Mfn2 are expressed relative to α -tubulin. *C*, MEFs from control and Mfn2-deficient MEFs were subjected to ER stress with 0.1 μ M TG or 0.5 μ g/ μ l TM for 18 h and immunoblotted for the ER chaperone proteins Grp94 and Grp78. *D*, quantitative real-time PCR was performed to determine the mRNA levels of *Mfn1*, *Mfn2*, *Opa1*, *Drp1*, *Fis1*, *ATF4*, and *Grp94*. Results are expressed as mean \pm S.E.; $n = 5$ /group; *, $p < 0.05$ versus TG or TM.

Thus, Mfn2 ablation does not affect the early TG- or TM-mediated increases in eIF2 α phosphorylation but delayed the dephosphorylation of eIF2 α that occurs at later time points. Consistent with this observation, Mfn2 ablation led to reductions in GADD34 and P58^{IPK} that promote eIF2 α dephosphorylation at the late time points (Fig. 6C). Quantitative analyses revealed that Mfn2 ablation led to 40.5 \pm 3.6% and 23.8 \pm 4.7% reductions in the level of GADD34 ($p < 0.05$), and 44.8 \pm 4.2% and 22 \pm 6.4% reductions in the level of P58^{IPK} ($p < 0.05$) in the TG- and TM-treated cells, respectively, at the 18-h time point. In contrast, loss of Mfn1 did not alter either UPR mediated PERK-eIF2 α phosphorylation or GADD34 and P58^{IPK} induction during late ER stress (Fig. 6E). Taken together, these data suggest that Mfn2 is induced during late UPR signaling and that this induction is essential for the dephosphorylation of eIF2 α and the induction of GADD34 and P58^{IPK}.

Loss of Mfn2 Leads to Maladaptive UPR and ER Stress-induced Cell Death—Prolonged ER stress will activate the expression of genes that contribute to the cell death program (37). Therefore, we tested whether loss of Mfn2 affects ER stress-induced apoptosis. Control and *AdCre*-treated Mfn2^{LoxP} MEFs were treated with TG or TM for 18 h, and cellular lysates were immunoblotted for CHOP or assayed for caspase 3/7 activity. Ablation of Mfn2 did not induce CHOP expression or affect caspase 3/7 activity at baseline. However, CHOP expression (Fig. 7A) and caspase activation (B) were significantly augmented by the loss of Mfn2 when ER stress was induced. Conversely, loss of Mfn1 did not affect either TG- or TM-mediated induction of CHOP (Fig. 7C).

To test whether loss of Mfn2 affects ER stress-induced cell viability, control and Mfn2-deficient MEFs were treated with TG or TM and stained with PI to assess cell death. The culture medium was also assayed for LDH release. In the absence of ER

Mfn2 and ER Stress

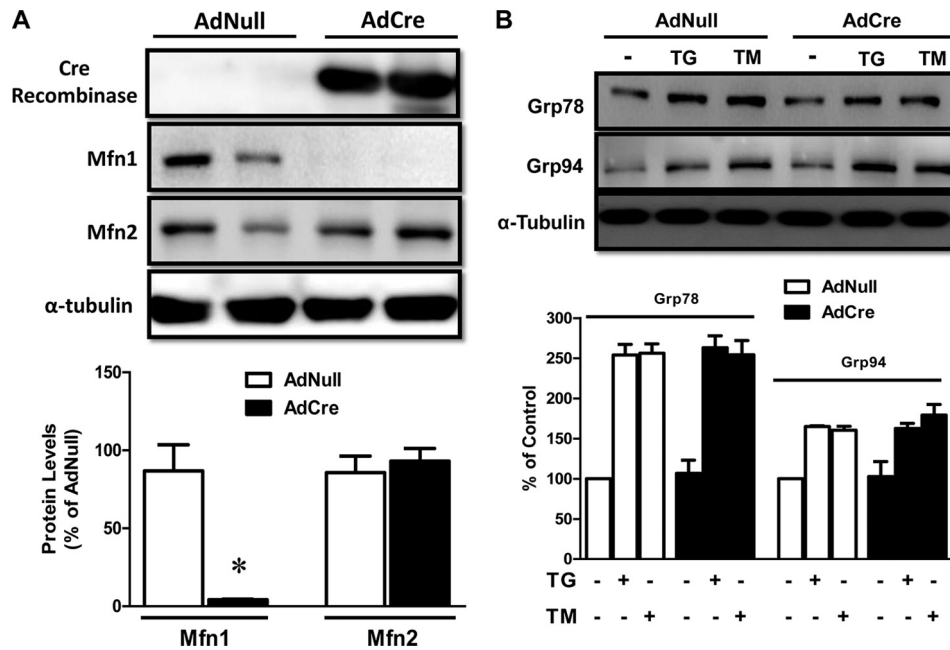


FIGURE 3. Loss of Mfn1 does not affect ER chaperone protein expression. LoXP-flanked Mfn1 MEFs were transfected with adenoviral vector-expressing Cre (*AdCre*) to delete Mfn1 or control virus (*AdNull*) for 72 h. *A*, whole cell lysates were immunoblotted for Cre recombinase, Mfn1, and Mfn2, and α -tubulin was used as a loading control. *B*, similarly treated MEFs were subjected to ER stress with 0.1 μ M TG or 0.5 μ g/ μ l TM for 18 h and were immunoblotted for the ER chaperone proteins Grp94 and Grp78. Results are expressed as mean \pm S.E.; $n = 5$ /group; *, $p < 0.05$ versus TG or TM.

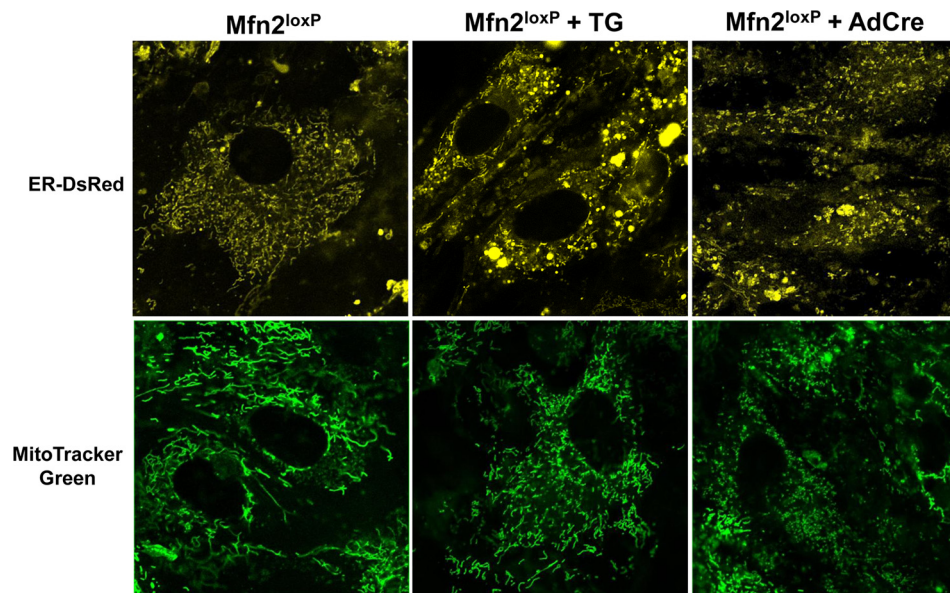


FIGURE 4. Loss of Mfn2 alters ER and mitochondrial morphology. LoXP-flanked Mfn2 MEFs transfected with an adenoviral vector-expressing Cre (*AdCre*) to delete Mfn2 or were treated with TG to induced ER stress. *Upper panels*, control, Mfn2-deficient, and TG-treated MEFs were transfected with a vector encoding the ER targeting sequence of calreticulin fused to DsRed2 and ER visualized using confocal microscopy. *Lower panels*, control, Mfn2-deficient and TG-treated MEFs were loaded with 100 nM MitoTracker Green, and mitochondria were visualized using confocal microscopy.

stress, Mfn2 ablation did not significantly alter these measures of cellular viability (Fig. 8, *A* and *B*). However, coupled with ER stress, loss of Mfn2 significantly increased the frequency of PI-positive nuclei (Fig. 8*A*) and increased LDH release into the media (*B*). In contrast, ablation of Mfn1 did not alter ER stress-induced PI-positivity (Fig. 8*C*).

DISCUSSION

This study examined the role of the mitochondrial fusion proteins Mfn1 and Mfn2 in the ER stress response. The data show that 1) pharmacologic induction of ER stress will up-reg-

ulate Mfn2 but not Mfn1 levels in MEFs; 2) deletion of Mfn2 but not Mfn1 in the heart or in MEFs up-regulates the expression of ER stress proteins; 3) loss of Mfn2 prolongs eIF2 α phosphorylation and diminishes the induction of GADD34 and P58^{IPK} in MEFs, indicative of an impairment in a recovery from translational repression; 4) ablation of Mfn2 augments ER stress-induced CHOP induction and caspase activation; 5) Mfn2 deficiency sensitizes MEFs to ER stress-induced death; and 6) unlike Mfn2 ablation, Mfn1 ablation did not affect the expression of ER stress proteins involved in translational recovery nor

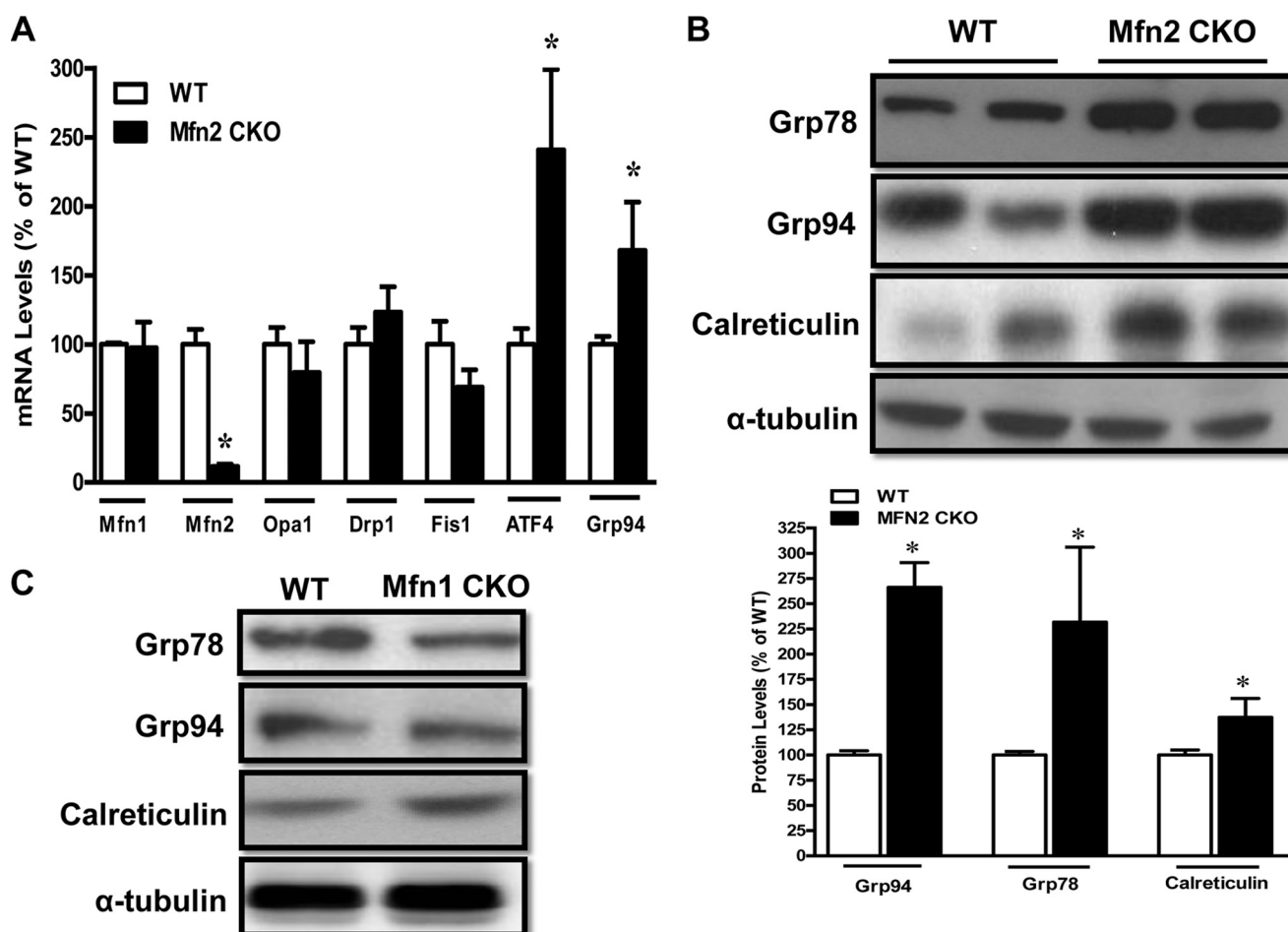


FIGURE 5. Cardiac myocyte-specific deletion of Mfn 2 but not Mfn 1 up-regulates ER chaperone expression *in vivo*. *A*, quantitative RT-PCR was performed on transcript-encoded cDNA isolated from WT and from Mfn2 CKO hearts to determine the mRNA levels of mitochondrial fusion proteins (*Mfn1*, *Mfn2*, and *Opa1*), mitochondrial fission proteins (*Drp1* and *Fis1*), activating transcription factor 4 (*ATF4*) and glucose-regulated protein 94 (*Grp94*). *B*, whole cell lysates isolated from hearts of wild-type mice or *Mfn2 CKO* were immunoblotted to detect endogenous levels of the ER chaperone proteins Grp94, Grp78, and calreticulin. Even though Mfn2 deletion in the heart did not significantly alter Mfn1 levels, it activated ER stress as reflected by immunoblot analyses showing augmented Grp94, Grp78, and calreticulin levels. Immunoblot analyses were quantified by densitometry, and GRP94, GRP78, and calreticulin levels are expressed relative to the α -tubulin loading control. *C*, Western blot analysis was performed to detect endogenous levels of Grp94, Grp78, and calreticulin in the heart of specific cardiac myocytes deletion of Mfn1 (*Mfn1 CKO*) relative to that in the wild type. Mfn1 deletion in the heart did not activate ER stress. Results are expressed as means \pm S.E. $n = 4-6$ /group; *, $p < 0.05$ versus WT.

ER stress-mediated CHOP induction and cell death. Thus, our study provides the first demonstration that Mfn2 is an ER stress-inducible protein that is required for the adaptation of the ER to stress.

We initially observed that inducers of ER stress led to the elevated expression of Mfn2. Mfn2 was induced by altering ER Ca^{2+} signaling with TG, inhibiting protein *N*-glycosylation with TM or by inhibiting the ER-Golgi trafficking of newly synthesized proteins through treatment with Brefeldin A (data not shown). Despite the differences in action of these pharmacological agents, the time course and extent of Mfn2 up-regulation was similar, suggesting that Mfn2 induction is a general feature of the ER stress response. This effect was highly specific for Mfn2, and the induction of ER stress had no effect on the expression of other mitochondrial shaping proteins including Mfn1, Opa1, Drp1, and Fis1. The specificity of Mfn2 induction by ER stress is particularly striking in light of the observation that ER stress is associated with marked changes in the morphology of the mitochondrial network (see Fig. 4). Finally, starvation (38), cold (39), and oxidative stress (40) have all been

reported to up-regulate Mfn2 expression. Because these stresses are also associated with the development of ER stress (41, 42), it is possible that the ER-mediated induction of Mfn2 is central to the regulation of this factor.

Like many other stress-induced signaling pathways, the UPR can exert both protective and detrimental effects on the cell (43). The strength and duration of the ER stress are critical determinants of whether the UPR exerts either a prosurvival or a prodeath signal. It is widely accepted that the initial UPR responses are oriented toward protection and the resolution of the ER stress. In contrast, UPR pathways activated late in ER stress can enhance apoptosis that is necessary for removal of irreversibly damaged cells (44, 45). In this regard, early and late UPR signals function in concert to temporally modulate translational activity. Early in ER stress, eIF2 α is inactivated by phosphorylation to suppress protein synthesis (46, 47). Later stages of the UPR require the synthesis of new stress-induced proteins, and eIF2 α is dephosphorylated through the actions of GADD34 and P58^{IPK} (22, 46, 47). Several groups have reported that excessive phosphorylation of eIF2 α leads to ATF4-medi-

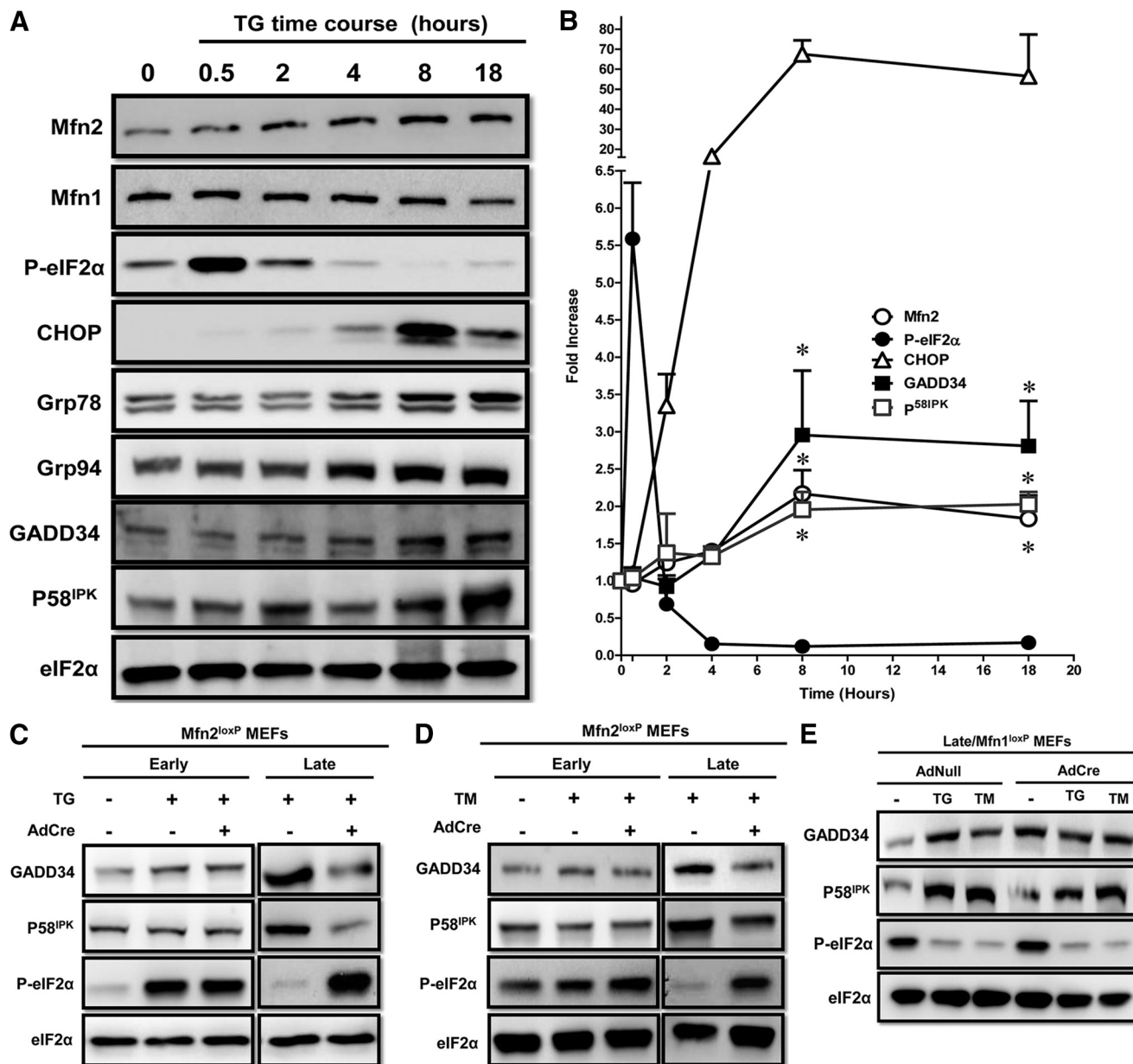


FIGURE 6. Loss of Mfn2 affects UPR signaling in a time-dependent manner. *A*, time courses of Mfn2 and of ER stress protein inducer in MEFs treated with 0.1 μ M TG for the indicated time points. *B*, densitometric quantification of time course of Mfn2 and ER stress proteins. *C*, control and Mfn2-deficient MEFs were treated with 0.1 μ M TG (0.5 or 18 h). Cell extracts were prepared from these cells and immunoblotted for phosphorylated eIF2 α , total eIF2 α , GADD34, and p58IPK. *D*, cell extracts from control and Mfn2-deficient MEFs treated with 0.5 μ g/ μ LTM for (1 or 18 h) were immunoblotted for phosphorylated eIF2 α , total eIF2 α , GADD34, and p58IPK. *E*, total cell extracts from control and Mfn1-deficient MEFs treated with 0.1 μ M TG or 0.5 μ g/ μ LTM for 18 h were immunoblotted for phosphorylated eIF2 α , total eIF2 α , GADD34, and p58IPK. Results are expressed as means \pm S.E. $n \geq 4$ /group. *, $p < 0.05$ versus TG or TM. CHOP induction is statistically significant at all time points. Phosphorylated eIF2 α (P-eIF2 α) levels differ from control at the 30 min, 4 h, 8 h, and 18 h time points ($p < 0.05$).

ated CHOP induction, resulting in apoptosis (10, 48). Here, it is shown that loss of Mfn2 does not affect the proximal effectors of the UPR, such as the rapid phosphorylation of eIF2 α . Instead, Mfn2 is up-regulated during the later stages of the ER stress response, and at these time points it appears to be required for the release from translational repression (Fig. 9). Consistent with this hypothesis, ablation of Mfn2 in MEFs led to prolonged eIF2 α phosphorylation and reductions in GADD34 and P58^{IPK} expression that serve to dephosphorylate and reactivate eIF2 α . Mfn2 ablation also led to a propagation of the proapoptotic UPR program, as indicated by CHOP induction and caspase activation, and led to greater cell death in response to ER stress.

CHOP is regulated by the ATF4 transcription factor, and ATF4 expression is enhanced by the phosphorylation of eIF2 α at Ser-51 (19). In agreement with these observations, we report that ATF4 expression is elevated in MEFs lacking Mfn2. Thus, it appears that the increased cell death caused by Mfn2 ablation is due to the activation of eIF2 α -ATF4-CHOP signaling, that may result from an impairment in the recovery from translational repression.

It is widely appreciated that both Mfn1 and Mfn2 control mitochondrial morphology by mediating the fusion of these organelles (49). It is also appreciated that mitochondria are juxtaposed with the ER. This close association is believed to be

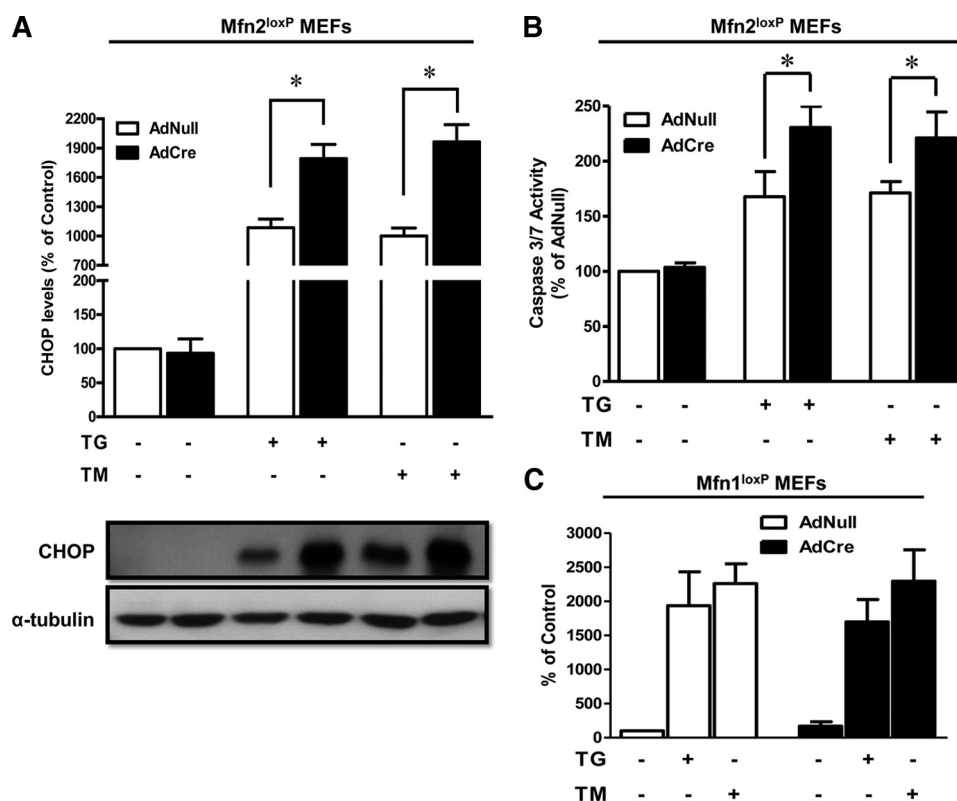


FIGURE 7. **Loss of Mfn2 activates the maladaptive UPR.** Total cell lysates from control and Mfn2-deficient MEFs were subjected to ER stress with 0.1 μM TG or 0.5 $\mu\text{g}/\mu\text{l}$ TM for 18 h and were immunoblotted for CHOP (A) or assayed for Caspase 3/7 activity (B). C, cell lysates from control and Mfn1-deficient MEFs subjected to ER stress with 0.1 μM TG or 0.5 $\mu\text{g}/\mu\text{l}$ TM for 18 h were immunoblotted for CHOP and α -tubulin. Blots were subjected to densitometry, and CHOP levels were quantified relative to α -tubulin expression. *, $p < 0.05$ versus TG or TM; $n = 4$ –6/group.

important in controlling lipid metabolism and Ca^{2+} transmission from the ER to the mitochondria (49). Recently, it has been shown that Mfn2 is present in the ER and that it tethers the ER and mitochondria (33). In the absence of Mfn2, ER structure is altered, and the distance between the ER and mitochondria is increased, diminishing mitochondrial Ca^{2+} uptake. Notably, Mfn1 was found to have no detectable role in controlling ER shape or ER-mitochondrial communication. Here, we show that Mfn2, but not Mfn1, is regulated by ER stress and has an essential role in the UPR program. Furthermore, ER stress and Mfn2 ablation promote similar morphological changes to both the mitochondrial and ER networks. Although these observations suggest that a dynamic interplay between mitochondria and the ER may be required for an appropriate UPR, further studies are required to discern whether or not the ER-mitochondria bridging function of Mfn2 mediates these actions on the UPR. In this regard, it has been reported that re-expression of Mfn2 with a mutation in the GTPase domain that causes Charcot-Marie-Tooth syndrome, or ablation of the p21-Ras binding domain, are sufficient to rescue the mitochondrial shape phenotype in Mfn2^{-/-} MEFs but have no effect on the altered ER morphology (33).

We also observed that cardiac myocyte-specific ablation of Mfn2, but not Mfn1, led to ER stress marker (e.g. Grp78, Grp94) expression in the heart. We have reported previously that Mfn2 ablation in cardiac myocytes leads to modest hypertrophy and only a small diminution in function when mice were stimulated with isoproterenol (29). In contrast to MEFs, ablation of Mfn2

in adult cardiac myocytes protected against cell death in response to a variety of stresses. In addition to having a proapoptotic role, ER stress can have a protective role in cardiac myocytes as well as other cell types through chaperone protein induction (50–52). In myocytes, ischemia will activate Grp78 expression via an ATF6-dependent mechanism, eliciting a preconditioning effect (53). It has also been reported that ER stress will activate autophagy in myocytes and promote cell survival (54). Thus, ER stress can fortify a cell against insults but can also lead to cell death, depending upon the strength and the duration of the ER stress. On the basis of these considerations, it is reasonable to speculate that the induction of chaperone proteins in the hearts of Mfn2 CKO mice contributes to their enhanced resistance to proapoptotic stresses.

In light of the above considerations, it should also be noted that studies report different effects of Mfn2-deficiency in different cell types (32, 55, 56). Discordant results with cardiac myocytes have also been reported. For example, Mfn2 ablation in cultured neonatal cardiac myocytes leads to cell death (57), whereas Mfn2 expression is reported to promote cell death in both neonatal cardiac myocytes and a cardiac myocyte cell line (40). In our own studies, we found that Mfn2-deficiency in cardiac myocytes protects the heart from ischemia-reperfusion injury, protects adult cardiac myocytes from oxidative stress-induced loss of mitochondrial membrane potential, and diminishes the sensitivity of mitochondria to undergo mitochondrial permeability transition (29). In contrast, we also found that siRNA knockdown of Mfn2 in cultured neonatal cardiac myo-

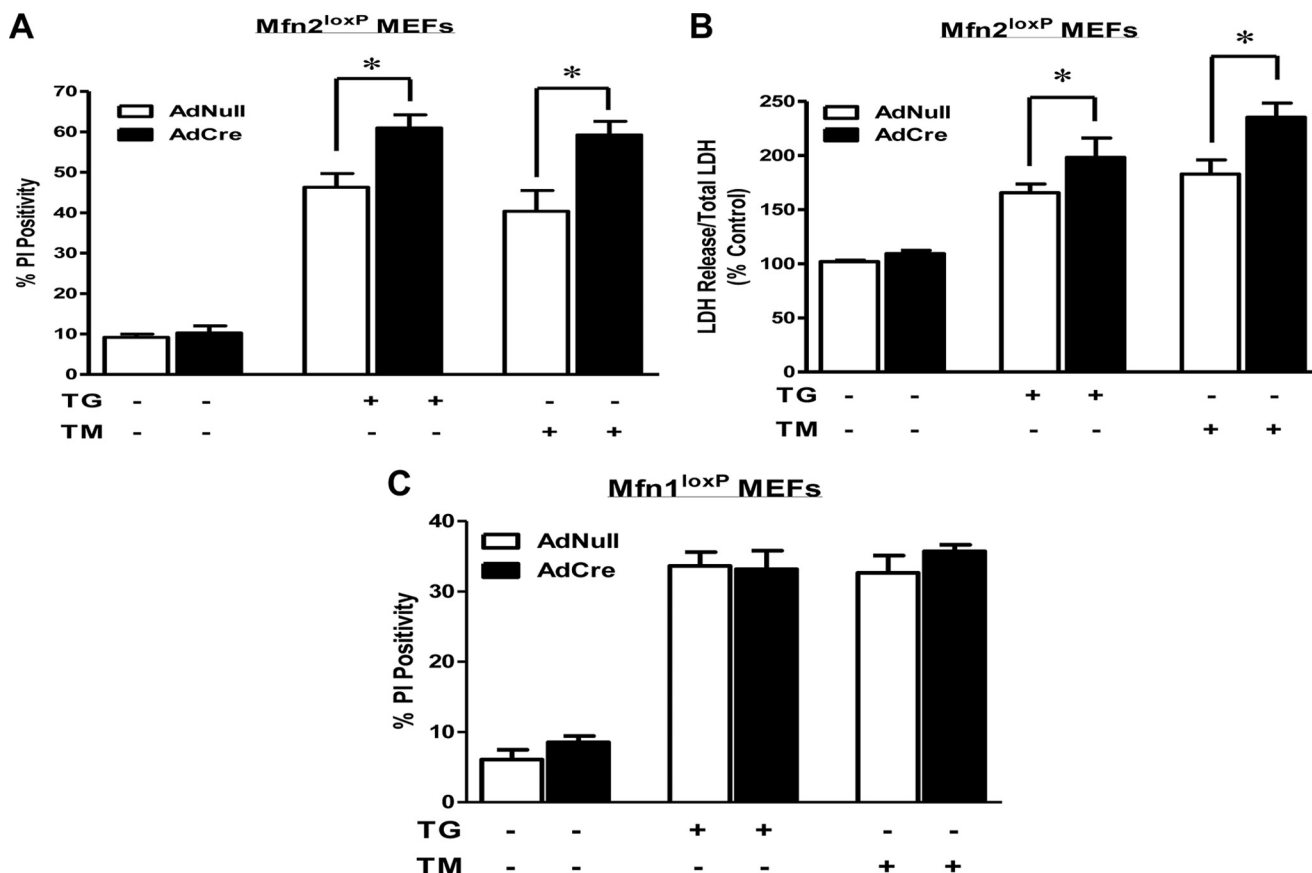


FIGURE 8. **Loss of Mfn2 sensitizes MEFs to ER stress-induced cell death.** *A*, control and Mfn2-deficient MEFs were treated with 0.1 μ M TG and 0.5 μ g/ μ L TM for 18 h and stained with DAPI and PI to evaluate cell death. *B*, the media from the same cultures were assayed for LDH release. *C*, control and Mfn1-deficient MEFs were treated with 0.1 μ M TG and 0.5 μ g/ μ L TM for 18 h and stained with DAPI and PI. Results are expressed as mean \pm S.E. $n = 4-6$ /group. *, $p < 0.05$ versus TG or TM.

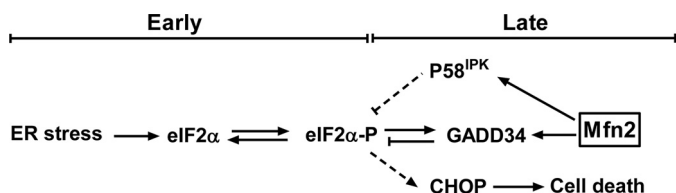


FIGURE 9. **Schematic model of the involvement of mitofusin 2 in UPR signaling.** *Cross arrows* indicate inhibition, whereas *other arrows* designate positive signaling. Under ER stress conditions, early UPR involves eIF2 α phosphorylation, leading to translational attenuation, whereas late UPR response involves GADD34- and P58IPK-mediated eIF2 α dephosphorylation and CHOP induction. Ablation of Mfn2 inhibits GADD34 and P58IPK expression, enhances CHOP induction, and promotes cell death.

cytes sensitized these cells to oxidative stress-induced loss of mitochondrial membrane potential and cell death (29). It is conceivable that these different effects of Mfn2 are due to differences in the quantity and organization of mitochondrial and, perhaps, ER networks within a particular cell type. For example, adult myocytes contain highly abundant mitochondria that are packed into a high ordered array that may favor the propagation of mitochondrial depolarizing events throughout the cell (58–61), thereby making these cells highly sensitive to cell death that is mediated by mechanisms that involve mitochondria. In contrast, neonatal myocytes are fibroblast-like and contain a much smaller number of mitochondria that are loosely organized within the cell. Thus, we speculate that the likelihood of a coordinated mitochondrial membrane depolarization is reduced in

neonatal myocytes and MEFs. In these cell types, other effects of Mfn2 ablation, such as the status of the pro- or antiapoptotic arms of the UPR, may predominate in the control of cell fate. Collectively, these data suggest that the actions of Mfn2 are likely to be highly dependent upon cellular context that can be influenced by the state of cellular differentiation, mitochondrial density, and, perhaps, the status of the ER.

In summary, we have identified Mfn2 as a new regulator of the ER stress response. We show that it is selectively up-regulated in response to ER stress, whereas other mitochondrial shaping proteins are not. Furthermore, we show that Mfn2 is essential for an appropriate elaboration of the UPR and ER homeostasis.

REFERENCES

1. Blobel, G. (2000) Protein targeting. *Biosci. Rep.* **20**, 303–344
2. Paschen, W. (2001) Dependence of vital cell function on endoplasmic reticulum calcium levels. Implications for the mechanisms underlying neuronal cell injury in different pathological states. *Cell Calcium* **29**, 1–11
3. Booth, C., and Koch, G. L. (1989) Perturbation of cellular calcium secretion induces secretion of luminal ER proteins. *Cell* **59**, 729–737
4. Kaufman, R. J. (1999) Stress signaling from the lumen of the endoplasmic reticulum. Coordination of gene transcriptional and translational controls. *Genes Dev.* **13**, 1211–1233
5. Schröder, M., and Kaufman, R. J. (2005) The mammalian unfolded protein response. *Annu. Rev. Biochem.* **74**, 739–789
6. Kozutsumi, Y., Segal, M., Normington, K., Gething, M. J., and Sambrook, J. (1988) The presence of malfolded proteins in the endoplasmic reticulum

- signals the induction of glucose-regulated proteins. *Nature* **332**, 462–464
7. Bertolotti, A., Zhang, Y., Hendershot, L. M., Harding, H. P., and Ron, D. (2000) Dynamic interaction of BiP and ER stress transducers in the unfolded-protein response. *Nat. Cell Biol.* **2**, 326–332
 8. Harding, H. P., Novoa, I., Zhang, Y., Zeng, H., Wek, R., Schapira, M., and Ron, D. (2000) Regulated translation initiation controls stress-induced gene expression in mammalian cells. *Mol. Cell* **6**, 1099–1108
 9. Szegezdi, E., Logue, S. E., Gorman, A. M., and Samali, A. (2006) Mediators of endoplasmic reticulum stress-induced apoptosis. *EMBO Rep.* **7**, 880–885
 10. Oyadomari, S., Araki, E., and Mori, M. (2002) Endoplasmic reticulum stress-mediated apoptosis in pancreatic β -cells. *Apoptosis* **7**, 335–345
 11. Delépine, M., Nicolino, M., Barrett, T., Golamaully, M., Lathrop, G. M., and Julier, C. (2000) EIF2AK3, encoding translation initiation factor 2- α kinase 3, is mutated in patients with Wolcott-Rallison syndrome. *Nat. Genet.* **25**, 406–409
 12. Zhou, J., Werstuck, G. H., Lhoták, S., de Koning, A. B., Sood, S. K., Hossain, G. S., Möller, J., Ritskes-Hoitinga, M., Falk, E., Dayal, S., Lentz, S. R., and Austin, R. C. (2004) Association of multiple cellular stress pathways with accelerated atherosclerosis in hyperhomocysteinemic apolipoprotein E-deficient mice. *Circulation* **110**, 207–213
 13. Katayama, T., Imaizumi, K., Honda, A., Yoneda, T., Kudo, T., Takeda, M., Mori, K., Rozmahel, R., Fraser, P., George-Hyslop, P. S., and Tohyama, M. (2001) Disturbed activation of endoplasmic reticulum stress transducers by familial Alzheimer's disease-linked presenilin-1 mutations. *J. Biol. Chem.* **276**, 43446–43454
 14. Dorner, A. J., Wasley, L. C., Raney, P., Haugejorden, S., Green, M., and Kaufman, R. J. (1990) The stress response in Chinese hamster ovary cells. Regulation of ERp72 and protein disulfide isomerase expression and secretion. *J. Biol. Chem.* **265**, 22029–22034
 15. Price, B. D., Mannheim-Rodman, L. A., and Calderwood, S. K. (1992) Brefeldin A, thapsigargin, and AIF4- stimulate the accumulation of GRP78 mRNA in a cycloheximide-dependent manner, whilst induction by hypoxia is independent of protein synthesis. *J. Cell. Physiol.* **152**, 545–552
 16. Ron, D., and Walter, P. (2007) Signal integration in the endoplasmic reticulum unfolded protein response. *Nat. Rev. Mol. Cell Biol.* **8**, 519–529
 17. Shen, J., Chen, X., Hendershot, L., and Prywes, R. (2002) ER stress regulation of ATF6 localization by dissociation of BiP/GRP78 binding and unmasking of Golgi localization signals. *Dev. Cell* **3**, 99–111
 18. Yoshida, H., Haze, K., Yanagi, H., Yura, T., and Mori, K. (1998) Identification of the cis-acting endoplasmic reticulum stress response element responsible for transcriptional induction of mammalian glucose-regulated proteins. Involvement of basic leucine zipper transcription factors. *J. Biol. Chem.* **273**, 33741–33749
 19. Scheuner, D., Song, B., McEwen, E., Liu, C., Laybutt, R., Gillespie, P., Saunders, T., Bonner-Weir, S., and Kaufman, R. J. (2001) Translational control is required for the unfolded protein response and *in vivo* glucose homeostasis. *Mol. Cell* **7**, 1165–1176
 20. Harding, H. P., Zhang, Y., and Ron, D. (1999) Protein translation and folding are coupled by an endoplasmic-reticulum-resident kinase. *Nature* **397**, 271–274
 21. Travers, K. J., Patil, C. K., Wodicka, L., Lockhart, D. J., Weissman, J. S., and Walter, P. (2000) Functional and genomic analyses reveal an essential coordination between the unfolded protein response and ER-associated degradation. *Cell* **101**, 249–258
 22. Yan, W., Frank, C. L., Korth, M. J., Sopher, B. L., Novoa, I., Ron, D., and Katze, M. G. (2002) Control of PERK eIF2 α kinase activity by the endoplasmic reticulum stress-induced molecular chaperone P58IPK. *Proc. Natl. Acad. Sci. U.S.A.* **99**, 15920–15925
 23. van Huizen, R., Martindale, J. L., Gorospe, M., and Holbrook, N. J. (2003) P58IPK, a novel endoplasmic reticulum stress-inducible protein and potential negative regulator of eIF2 α signaling. *J. Biol. Chem.* **278**, 15558–15564
 24. Santel, A., and Fuller, M. T. (2001) Control of mitochondrial morphology by a human mitofusin. *J. Cell Sci.* **114**, 867–874
 25. Chen, H., Detmer, S. A., Ewald, A. J., Griffin, E. E., Fraser, S. E., and Chan, D. C. (2003) Mitofusins Mfn1 and Mfn2 coordinately regulate mitochondrial fusion and are essential for embryonic development. *J. Cell Biol.* **160**, 189–200
 26. Züchner, S., Mersyanova, I. V., Muglia, M., Bissar-Tadmouri, N., Rochelle, J., Dadali, E. L., Zappia, M., Nelis, E., Patitucci, A., Senderek, J., Parman, Y., Evgrafov, O., Jonghe, P. D., Takahashi, Y., Tsuji, S., Pericak-Vance, M. A., Quattrone, A., Battaloglu, E., Polyakov, A. V., Timmerman, V., Schröder, J. M., and Vance, J. M., and Battaloglu, E. (2004) Mutations in the mitochondrial GTPase mitofusin 2 cause Charcot-Marie-Tooth neuropathy type 2A. *Nat. Genet.* **36**, 449–451
 27. Chen, H., McCaffery, J. M., and Chan, D. C. (2007) Mitochondrial fusion protects against neurodegeneration in the cerebellum. *Cell* **130**, 548–562
 28. Chen, H., Vermulst, M., Wang, Y. E., Chomyn, A., Prolla, T. A., McCaffery, J. M., and Chan, D. C. (2010) Mitochondrial fusion is required for mtDNA stability in skeletal muscle and tolerance of mtDNA mutations. *Cell* **141**, 280–289
 29. Papanicolaou, K. N., Khairallah, R. J., Ngoh, G. A., Chikando, A., Luptak, I., O'Shea, K. M., Riley, D. D., Lugus, J. J., Colucci, W. S., Lederer, W. J., Stanley, W. C., and Walsh, K. (2011) Mitofusin-2 maintains mitochondrial structure and contributes to stress-induced permeability transition in cardiac myocytes. *Mol. Cell Biol.* **31**, 1309–1328
 30. Papanicolaou, K. N., Ngoh, G. A., Dabkowski, E. R., O'Connell, K. A., Ribeiro, R. F., Jr., Stanley, W. C., and Walsh, K. (2012) Cardiomyocyte deletion of mitofusin-1 leads to mitochondrial fragmentation and improves tolerance to ROS-induced mitochondrial dysfunction and cell death. *Am. J. Physiol. Heart Circ. Physiol.* **302**, H167–179
 31. Chen, Y., Liu, Y., and Dorn, G. W., 2nd. (2011) Mitochondrial fusion is essential for organelle function and cardiac homeostasis. *Circ. Res.* **109**, 1327–1331
 32. de Brito, O. M., and Scorrano, L. (2008) Mitofusin 2. A mitochondria-shaping protein with signaling roles beyond fusion. *Antioxid. Redox Signal.* **10**, 621–633
 33. de Brito, O. M., and Scorrano, L. (2008) Mitofusin 2 tethers endoplasmic reticulum to mitochondria. *Nature* **456**, 605–610
 34. Kamijo, T., Zindy, F., Roussel, M. F., Quelle, D. E., Downing, J. R., Ashmun, R. A., Grosveld, G., and Sherr, C. J. (1997) Tumor suppression at the mouse INK4a locus mediated by the alternative reading frame product p19ARF. *Cell* **91**, 649–659
 35. Ngoh, G. A., Facundo, H. T., Hamid, T., Dillmann, W., Zachara, N. E., and Jones, S. P. (2009) Unique hexosaminidase reduces metabolic survival signal and sensitizes cardiac myocytes to hypoxia/reoxygenation injury. *Circ. Res.* **104**, 41–49
 36. Ngoh, G. A., Hamid, T., Prabhu, S. D., and Jones, S. P. (2009) O-GlcNAc signaling attenuates ER stress-induced cardiomyocyte death. *Am. J. Physiol. Heart Circ. Physiol.* **297**, H1711–1719
 37. Xu, C., Bailly-Maitre, B., and Reed, J. C. (2005) Endoplasmic reticulum stress. Cell life and death decisions. *J. Clin. Invest.* **115**, 2656–2664
 38. Li, Y., Yin, R., Liu, J., Wang, P., Wu, S., Luo, J., Zhelyabovska, O., and Yang, Q. (2009) Peroxisome proliferator-activated receptor delta regulates mitofusin 2 expression in the heart. *J. Mol. Cell Cardiol.* **46**, 876–882
 39. Soriano, F. X., Liesa, M., Bach, D., Chan, D. C., Palacín, M., and Zorzano, A. (2006) Evidence for a mitochondrial regulatory pathway defined by peroxisome proliferator-activated receptor- γ coactivator-1 α , estrogen-related receptor- α , and mitofusin 2. *Diabetes* **55**, 1783–1791
 40. Shen, T., Zheng, M., Cao, C., Chen, C., Tang, J., Zhang, W., Cheng, H., Chen, K. H., and Xiao, R. P. (2007) Mitofusin-2 is a major determinant of oxidative stress-mediated heart muscle cell apoptosis. *J. Biol. Chem.* **282**, 23354–23361
 41. Paul, P. K., Bhatnagar, S., Mishra, V., Srivastava, S., Darnay, B. G., Choi, Y., and Kumar, A. (2012) The E3 ubiquitin ligase TRAF6 intercedes in starvation-induced skeletal muscle atrophy through multiple mechanisms. *Mol. Cell Biol.* **32**, 1248–1259
 42. Liu, H., Bowes, R. C., 3rd, van de Water, B., Sillence, C., Nagelkerke, J. F., and Stevens, J. L. (1997) Endoplasmic reticulum chaperones GRP78 and calreticulin prevent oxidative stress, Ca²⁺ disturbances, and cell death in renal epithelial cells. *J. Biol. Chem.* **272**, 21751–21759
 43. Bernales, S., Papa, F. R., and Walter, P. (2006) Intracellular signaling by the unfolded protein response. *Annu. Rev. Cell Dev. Biol.* **22**, 487–508
 44. Silva, R. M., Ries, V., Oo, T. F., Yarygina, O., Jackson-Lewis, V., Ryu, E. J., Lu, P. D., Marciniak, S. J., Ron, D., Przedborski, S., Kholodilov, N., Greene,

- L. A., and Burke, R. E. (2005) CHOP/GADD153 is a mediator of apoptotic death in substantia nigra dopamine neurons in an *in vivo* neurotoxin model of parkinsonism. *J. Neurochem.* **95**, 974–986
45. Zinszner, H., Kuroda, M., Wang, X., Batchvarova, N., Lightfoot, R. T., Remotti, H., Stevens, J. L., and Ron, D. (1998) CHOP is implicated in programmed cell death in response to impaired function of the endoplasmic reticulum. *Genes Dev.* **12**, 982–995
46. Ma, Y., and Hendershot, L. M. (2003) Delineation of a negative feedback regulatory loop that controls protein translation during endoplasmic reticulum stress. *J. Biol. Chem.* **278**, 34864–34873
47. Kojima, E., Takeuchi, A., Haneda, M., Yagi, A., Hasegawa, T., Yamaki, K., Takeda, K., Akira, S., Shimokata, K., and Isobe, K. (2003) The function of GADD34 is a recovery from a shutoff of protein synthesis induced by ER stress. Elucidation by GADD34-deficient mice. *FASEB J.* **17**, 1573–1575
48. Cnop, M., Ladriere, L., Hekerman, P., Ortis, F., Cardozo, A. K., Dogusan, Z., Flamez, D., Boyce, M., Yuan, J., and Eizirik, D. L. (2007) Selective inhibition of eukaryotic translation initiation factor 2 α dephosphorylation potentiates fatty acid-induced endoplasmic reticulum stress and causes pancreatic beta-cell dysfunction and apoptosis. *J. Biol. Chem.* **282**, 3989–3997
49. de Brito, O. M., and Scorrano, L. (2010) An intimate liaison. Spatial organization of the endoplasmic reticulum-mitochondria relationship. *EMBO J.* **29**, 2715–2723
50. Zhang, P. L., Lun, M., Teng, J., Huang, J., Blasick, T. M., Yin, L., Herrera, G. A., and Cheung, J. Y. (2004) Preinduced molecular chaperones in the endoplasmic reticulum protect cardiomyocytes from lethal injury. *Ann. Clin. Lab. Sci.* **34**, 449–457
51. Peyrou, M., and Cribb, A. E. (2007) Effect of endoplasmic reticulum stress preconditioning on cytotoxicity of clinically relevant nephrotoxins in renal cell lines. *Toxicol. In Vitro* **21**, 878–886
52. Cybulsky, A. V., Takano, T., Papillon, J., Kitzler, T. M., and Bijian, K. (2011) Endoplasmic reticulum stress in glomerular epithelial cell injury. *Am. J. Physiol. Renal Physiol.* **301**, F496–508
53. Doroudgar, S., Thuerauf, D. J., Marcinko, M. C., Belmont, P. J., and Glembofski, C. C. (2009) Ischemia activates the ATF6 branch of the endoplasmic reticulum stress response. *J. Biol. Chem.* **284**, 29735–29745
54. Gustafsson, A. B., and Gottlieb, R. A. (2008) Recycle or die. The role of autophagy in cardioprotection. *J. Mol. Cell Cardiol.* **44**, 654–661
55. Sack, M. N. (2011) Mitofusin function is dependent on the distinct tissue- and organ-specific roles of mitochondria. *J. Mol. Cell Cardiol.* **51**, 881–882
56. Lugas, J. J., Ngoh, G. A., Bachschmid, M. M., and Walsh, K. (2011) Mitofusins are required for angiogenic function and modulate different signaling pathways in cultured endothelial cells. *J. Mol. Cell Cardiol.* **51**, 885–893
57. Parra, V., Eisner, V., Chiong, M., Criollo, A., Moraga, F., Garcia, A., Härtel, S., Jaimovich, E., Zorzano, A., Hidalgo, C., and Lavandero, S. (2008) Changes in mitochondrial dynamics during ceramide-induced cardiomyocyte early apoptosis. *Cardiovasc. Res.* **77**, 387–397
58. Aon, M. A., Cortassa, S., Marbán, E., and O'Rourke, B. (2003) Synchronized whole cell oscillations in mitochondrial metabolism triggered by a local release of reactive oxygen species in cardiac myocytes. *J. Biol. Chem.* **278**, 44735–44744
59. Brady, N. R., Elmore, S. P., van Beek, J. J., Krab, K., Courtoy, P. J., Hue, L., and Westerhoff, H. V. (2004) Coordinated behavior of mitochondria in both space and time. A reactive oxygen species-activated wave of mitochondrial depolarization. *Biophys. J.* **87**, 2022–2034
60. Brady, N. R., Hamacher-Brady, A., Westerhoff, H. V., and Gottlieb, R. A. (2006) A wave of reactive oxygen species (ROS)-induced ROS release in a sea of excitable mitochondria. *Antioxid. Redox. Signal* **8**, 1651–1665
61. Zorov, D. B., Filburn, C. R., Klotz, L. O., Zweier, J. L., and Sollott, S. J. (2000) Reactive oxygen species (ROS)-induced ROS release. A new phenomenon accompanying induction of the mitochondrial permeability transition in cardiac myocytes. *J. Exp. Med.* **192**, 1001–1014